FOURTH AUSTRALASIAN CONFERENCE
on
HYDRAULICS AND FLUID MECHANICS
at
Monash University, Melbourne, Australia
1971 November 29 to December 3

TRANSPORT PHENOMENON IN A LABORATORY WIND WAVE CHANNEL: I. COMPARISON OF TWO SHEAR PREDICTION METHODS UNDER ISOTHERMAL CONDITIONS

by

A. JOHN CHAMBERS
PETER A. MANGERELLA
ROBERT L. STREET
EN YUN HSU

An experimental program was conducted at Stanford University to examine the heat, mass and momentum transfer close to a water surface. From the data taken during this program, surface transfer coefficients of heat, mass and shear were determined.

This article restricts the discussion to momentum results taken under isothermal conditions. Comparison is made between two shear stress prediction methods: namely, the profile and the integral methods.

It was found that the integral surface shear values are more consistent with the flow field than those given by the profile method. The profile method is thought to overpredict surface shear because it is not applied correctly (it is applied in a region where the 'law of the wall' is not applicable, no corrections are made for zero displacement, and because of the necessity to obtain two parameters from the curve fit).

J. Chambers, Drexel University
P. Mangarella, University of Massachusetts
R. Street, Stanford University
E. Hsu, Stanford University

Recently an experimental program was conducted at Stanford University to examine heat mass and momentum transfer close to a water interface (1,7). Profiles of average velocity, temperature and humidity were measured at various stations in the Stanford Wind Water Research Facility. All these profiles were taken in the air. Measurements of the surface properties of water were also made. From this data, surface transfer coefficients of heat, mass and shear were determined.

It is intended to restrict the discussion in this article to the momentum results taken under isothermal conditions and to point out what the authors feel is an interesting conflict in the results of two prediction methods used to obtain shear stress coefficients.

For these experiments three specific surface conditions were considered: air flow over a solid surface, air flow over a water surface (wind-generated waves only) and air flow over a water surface with a mechanically-generated wave (swell and wind-generated waves). This discussion will be restricted to the air flow over a water surface with wind-generated waves only. Four different free stream air velocities were considered, namely 3.6 m/sec, 6.8 m/sec, 11.0 m/sec, and 15.0 m/sec.

Shear Stress Determination Methods

It is customary to express the surface drag τ_0 at an air-water boundary in terms of the shear stress coefficient C_z, air density ρ, and the mean wind speed U specified at some height z above the surface; thus,

$$\tau_0 = \rho C_z U_z^2 \tag{1}$$

The coefficient C_z is also known as the resistance, drag or friction coefficient. By the nature of this definition the drag coefficient depends on the height at which the velocity is specified. For field measurements this height is usually taken as 10 m. Laboratory measurements may use the free stream velocity or the velocity at a height, for example, of 10 cm when specifying C_z. For this study the shear-stress coefficient will be defined as

$$C_f = \frac{\tau_0}{\rho U_\infty^2} \tag{2}$$

where U_∞ is the free stream velocity.

A summary of the various field and laboratory methods of estimating the friction coefficient is given by Roll (9). For this study the following two methods were used:

a) Application of the conservation of horizontal momentum principle where the boundary shear is expressed as a function of observable differences or integral terms (a budget method).

b) Use of the vertical profile of mean horizontal wind velocity and Prandtl's assumed form of the profile slope (profile method).

Integral Method

The essential feature of an integral shear stress determination method is that it is necessary to balance inflow and outflow parameters on a control volume. For a two-dimensional boundary layer flow it may be established by dimensional reasoning that $\frac{\partial P}{\partial z} = 0$ and that $\frac{\partial P}{\partial x} \simeq \frac{dP}{dx}$ (11). Now it is possible to determine the two-dimensional horizontal momentum integral equation by use of a method similar to Kays (5). The result one obtains is derived by Chambers, et.al,(1) namely:

$$C_f = \frac{d\delta_2}{dx} + \frac{1}{U_\infty}\frac{dU_\infty}{dx}(2\delta_2 + \delta_1) - F_b\left(\frac{U_\infty - U_0}{U_\infty}\right) \tag{3}$$

where δ_1 is the displacement thickness of the momentum boundary layer

$$\delta_1 \triangleq \int_0^Z \left(1 - \frac{\rho U}{\rho_\infty U_\infty}\right) dz \tag{4}$$

δ_2 is the momentum thickness of the boundary layer

$$\delta_2 \triangleq \int_0^Z \frac{\rho U}{\rho_\infty U_\infty}\left(1 - \frac{U}{U_\infty}\right) dz \tag{5}$$

and F_b is the blowing fraction

$$F_b = \frac{\rho_0 V_0}{\rho_\infty U_\infty} \tag{6}$$

The distance Z is chosen to extend into the potential flow region. Uo is the component of velocity along the channel at the interface and Vo is the normal component of velocity.

For this study the density was essentially constant (isothermal conditions). Before C_f can be computed it is necessary to compute the integral parameters δ_1 and δ_2. The contribution of integral parameters in the region above the lowest velocity measurement was determined from the defining equations, Eqs. 4 and 5 by application of the trapezoidal rule. The contribution below this level was obtained by extrapolating the lower portion of the measured profile to the mean water surface. A semilog form (U/U_∞ versus log z) for the extrapolation was used. For some of the cases studied the extrapolated zone contributed as much as 50 percent of the value of the integral parameter.

The right side of Eq. (3) was evaluated from the experimental data. Average vertical profiles of velocity above the surface were taken consecutively from Stations 3 to 10. The displacement and momentum thicknesses were evaluated for each station. The momentum thickness data were smoothed using a second-order curve fitted by a least-squares technique. The gradient of δ_2 was then computed from this curve. The pressure gradient term was determined by smoothing the free stream velocity in a similar manner as that used for the momentum thickness. The blowing fraction F_b was supplied from the results of Mangarella, et. al.(7).

Profile Method for Air-Water Interface Flows

The sheared velocity profile over water waves is commonly given in the form (10)

$$\frac{U}{u_*} = \frac{1}{\kappa} \ln \frac{z}{z_0} \tag{7}$$

where z_0 is the "aerodynamic roughness" of the water surface, z is a distance measured from the mean water level, $u_* = (\frac{\tau_o}{\rho})^{1/2}$ is the friction velocity, and κ is the universal von Karman constant (for this study $\kappa = 0.40$).

The form of the velocity profile over water is given by Eq. (7). Plots of U/U_∞ versus log z indicated that at least the nine data points closest to the boundary were in a log-linear region. A straight line was fitted to the lower nine profile points using a least-squares technique. The value of u_* comes directly from the slope and z_0 from the intercept of the fitted line with U = 0.

THE WIND, WATER-WAVE RESEARCH FACILITY AND INSTRUMENTATION

The facility has cross-sectional dimensions of 1.93 m high by 0.91 m wide. The overall length is 35 m with a glass test section of about 20 m. The cross-sectional area varies by about 1 percent along the test section. A schematic view of the arrangement of the facility is shown in Fig. 1. For further structural features see Hsu (4). For the present tests the water depth in the channel was 0.96 m, leaving 0.97 m for the vertical depth of the air flow.

Situated at one end of the channel is a wave generating plate rigidly connected to a hydraulic cylinder which is linked to a servo-control system. The signal from a function generator, with a frequency resolution of ±1 percent, forms the input to the servo-system for the generation of a progressive wave train. At the other end of the channel is a beach which absorbs wave energy. The beach consists of stainless steel turnings packed in expanded metal-covered baskets. The baskets are mounted on boards supported on a steel frame which provides a 1 on 5 sloping face.

Just above and behind the beach is a centrifugal, airfoil-bladed fan with control systems designed to hold drift to ±1 RPM. An air-straightening vane consisting of a 10.2 cm thick stainless steel honeycomb with 0.476 cm cells prevents the vortex motion created by the fan from extending upstream into the channel test section. Located 5.18 m downstream of the mean position

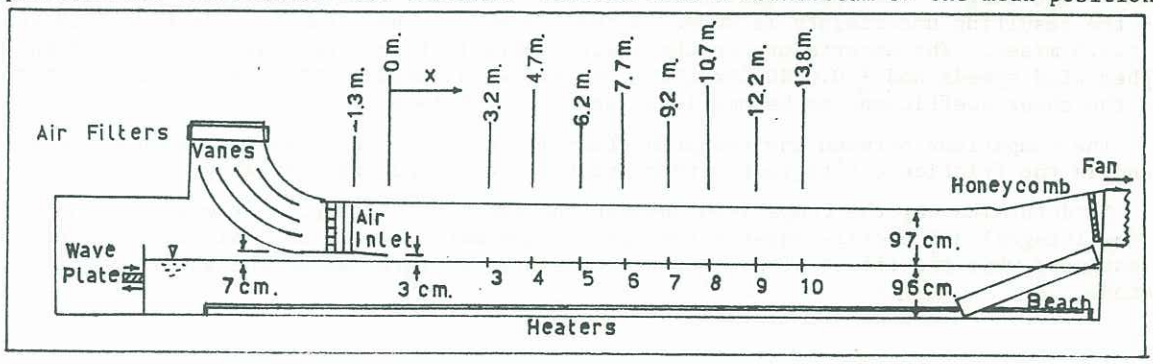

Fig. 1 - Schematic View of Stanford Wind, Water-Wave Facility

of the wave generating plate is the air inlet. Air is sucked through a system of fiberglass furnace filters into a converging elbow partitioned by three turning vanes. The turning vanes minimize the nonuniformity of the entering air stream. The flow then passes through a straightening vane made of honeycomb and then through two smoothing screens of 0.32 cm. mesh before entering the test section.

Experimental Configuration

A short smooth sloping plate was attached at the air inlet. To allow a mechanically-generated wave of 3.2 cm wave height to propagate into the test section the mean water surface was set 3 cm below the downstream edge of the sloping plate. The lowest point on the sloping plate was just below the ribbing forming the lower support for the screens attached to the air inlet.

A distance of about 3 m from the end of the sloping plate was necessary for the flow to reattach itself and settle down. The first location for data taking was 3.2 m downstream from the end of the sloping plate. This became known as Station 3. Initially stations were located at the end of this plate and midway between that position and Station 3; the space between stations was about 1.5 m. For the exact spacing see Fig. 1.

Mean Air Velocity

Mean air velocities were obtained from the pressure differential of a pitot-static probe. The probe was 0.24 cm outside diameter and 0.12 cm inside diameter. The probe is a standard shelf item manufactured by United Sensors and Control Corporation.

A Pace differential-pressure transducer (Model P90D) with a full range of $\pm$ 2.12 cm of water was used to measure the pressure differential from the pitot-static probe. A Sanborn Model 650 carrier-amplifier system was coupled to the pressure transducer. Static calibrations of the transducer and the recording system were obtained using a Combust micromanometer which indicated differential head with a resolution of $\pm$ 0.0006 cm of fluid of specific gravity 0.82.

The calibration curves were checked from time to time during experimental runs and the maximum deviation of this slope from that of an earlier calibration was 1.7 percent. Generally the deviation was less than 0.5 percent.

Probe Support Mechanism

A motorized traverse and position indicator permitted remote control of probe location in the longitudinal, horizontal and vertical planes within the wind wave facility. Velocity probes were located at two levels on the vertical traverse. The vertical distance between the two pitot probes was approximately 29 cm. In all experimental runs the lower set of probes traversed beyond the boundary-affected region into a core region.

RESULTS AND DISCUSSION OF RESULTS

Fig. 2 shows the variation of the drag or shear coefficient C_f with fetch. Also shown is the comparison between the profile method and integral method of shear determination.

The solid lines represent the integral results, the actual computed points falling very close to these lines. Shown on the line for $U_\infty \simeq 15.0$ m/sec is a vertical bar representing the uncertainty in the integral shear stress coefficient. This uncertainty value indicates a range of $\pm$ 0.0004 in the shear stress coefficient for a given velocity and is the same for all free stream velocities. The blowing term (Eq. 3) was obtained from the results of Mangarella, et. al. (6) and in all cases was small ($\simeq$ 0.00005). The pressure gradient term

$$(2\delta_2 + \delta_1) \frac{1}{U_\infty} \frac{dU_\infty}{dx}$$

is larger and accounts for approximately 30 percent of the shear coefficient value. In all cases the integral shear coefficient decreased as the fetch x was increased.

The profile results are represented by squares in Fig. 2 and in all cases the scatter in the results was large. The RMS variation on the profile shear coefficient was obtained for each run and the resulting uncertainty is shown on the figure as a vertical bar for $U_\infty \simeq 15.0$ and $U_\infty \simeq 3.5$ m/sec. The uncertainty on the shear coefficient obtained was $\pm$ 0.0012 for the two higher wind speeds and $\pm$ 0.0010 for the lower two wind speeds. The trend in the profile data is for the shear coefficient to become lower as the fetch is increased.

The comparison between the two prediction methods is poor. However, both exhibit a similar trend in the friction coefficient with respect to fetch and free stream velocity.

To determine why the comparison between the two methods is poor, the underlying assumptions of the integral and profile shear stress prediction methods will be examined. An attempt is made to estimate what the effect of neglecting certain parameters has on the shear coefficients predicted.

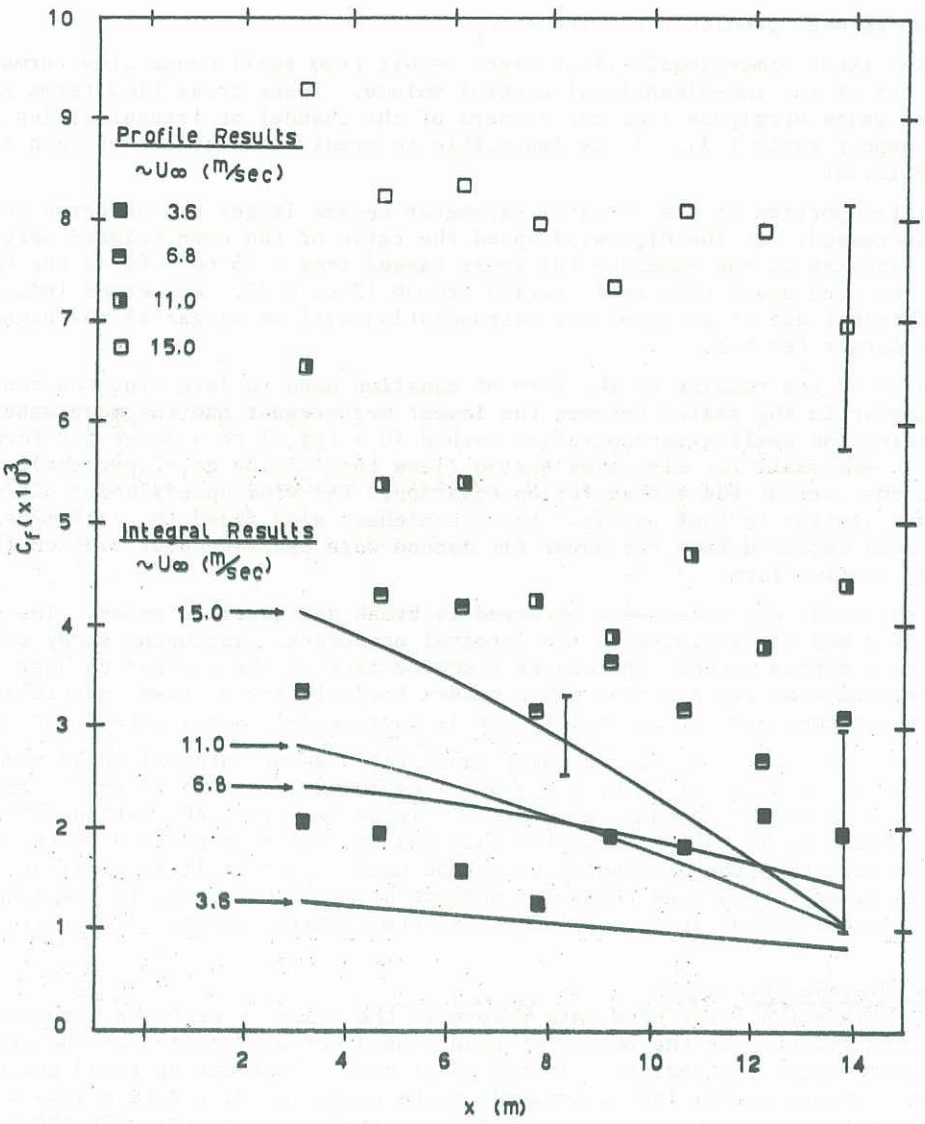

Fig. 2 - Comparison of Integral and Profile Shear Stress Coefficients

Qualifications of Integral Procedure

The two-dimensional momentum integral equation (3) is modified if three-dimensional effects are incorporated in the model. The horizontal momentum integral equation at the plane of symmetry for a three dimensional flow, in which no boundary layer skewing occurs (the streamlines have zero curvature), was derived by Schlichting (11) as

$$C_f = \frac{\partial \delta_2}{\partial x} + (2\delta_2 + \delta_1) \frac{1}{U_\infty} \frac{\partial U_\infty}{\partial x} + \frac{\delta_2}{A} \qquad (8)$$

where A is the distance from a point in the flow to the virtual origin of the streamlines.

In the case of flow over a solid boundary the displacement thickness grows linearly with x. A similar rate of growth of δ_1 would be expected on the side walls; thus, effects caused by streamline skewing will be negligible because δ_1 represents the effective flow blockage due to boundary layer growth and thus the streamlines will be converging towards a point. It was found that δ_1 increased approximately 1 cm in 10 m; thus, A $\simeq$ -450 m. It appears from this analysis that possible three-dimensional flow conditions at the plane of symmetry have a negligibly small effect on the shear stress coefficient in the present study.

Another error introduced by three-dimensional effects is that of side shear forces acting on the control volume. Examining a velocity profile taken across the channel shows that a maximum occurs near the center of the channel. This curvature of the velocity profile indicates that there is a component of shear stress ($\overline{\rho uw} = K_m \frac{\partial U}{\partial y}$) acting on the sides of the control volume. For equation 3 this stress is assumed zero. The side stress acts in the same direction as the bottom shear τ_0 because the flow in the control volume is being retarded by the neighboring flow. Thus, the effect of including side-shear would be to increase the apparent bottom-shear stress coefficient calculated by a two-dimensional method. Neglecting side-shear forces will cause the

integral technique to over predict the value of C_f.

The only other three-dimensional effect might result from small cross flow terms convecting momentum into or out of the two-dimensional control volume. These cross flow terms may be caused by vortices which originate from the corners of the channel or irregularities in the flow due to the small aspect ratio (≈1). It is impossible to predict the effect of such terms on the shear stress coefficient.

The extrapolated portion of the integral parameter became larger as the fetch increased and as the velocity increased. At the high wind speed the ratio of the extrapolated portion of the momentum thickness to the momentum thickness ranged from 0.45 to 0.60 as the fetch increased. At the low wind speed this ratio varied from 0.12 to 0.20. Any error induced in the shear stress coefficient due to an incorrect extrapolation will be larger at the higher wind speeds and at the larger fetches.

The sensitivity of the results to the form of equation used to determine the contribution to the integral parameter in the region between the lowest measurement and the mean water level was obtained by comparing the semilog extrapolation method ($U \alpha \log z$) to a power fit form ($U \alpha z^a$). The variation in δ_2 was small for all cases tested (less than $\pm$ 0.04 cm, 2 percent); δ_1 was more sensitive to the form of the extrapolation equation. For wind speeds below 6.8 m/sec the variation in δ_1 was similar to that for δ_2. For the highest wind speed ($U_\infty \approx$ 15 m/sec) the displacement thicknesses obtained from the power fit method were usually about 0.35 cm (12 percent) lower than for the semilog form.

At higher wind speeds the waves were observed to break and generate spray. The effect of spray on surface drag was not included in the integral procedure. Including spray effects in the two-dimensional momentum method, introduces a source term to the control volume. The spray particles take momentum from the air flow which causes the velocity of these particles to increase. Thus, the apparent bottom-shear stress coefficient is increased if spray effects are neglected.

It must be concluded that the effects which cause the present integral shear results to increase (so that they match those given by the profile estimates) are due to small cross flow terms and extrapolation errors in the integral parameters. It is felt that the extrapolation errors will have a minor effect as it was demonstrated that the extrapolated portion of the momentum thickness is not sensitive to the extrapolation method used. Further, it is difficult to believe that errors induced by any cross flow terms (if present at all) would lead to the large differences in the prediction methods. Thus it is concluded that the integral method gives reliable estimates of shear stress.

Evaluation of Profile Technique

Over a water surface the lower nine data points in the velocity profiles were used to obtain the shear stress coefficient. As the number of points used for application of the profile method was varied from five to nine the variation in the shear coefficient was up to 40 percent (Fig. 3). Generally, the shear stress coefficient increased as the number of U, z data points to C_f were increased. This sensitivity to the number of points required to adequately fit the data is reflected in the uncertainties of the profile shear coefficient (Fig. 3). In all cases the velocity profiles appeared linear with log z in the region fitted. The regions fitted were $z/\delta < 0.65$ for $U_\infty \approx$ 15 m/sec, $z/\delta < 0.5$ for $U_\infty \approx$ 11.0 m/sec, and $z/\delta < 0.4$ for $U_\infty \approx$ 6.8 m/sec and $U_\infty \approx$ 3.6 m/sec. δ is the boundary layer thickness. In Fig. 3 $z/\delta \approx 0.2$ occurs between the third and fourth U, z data points.

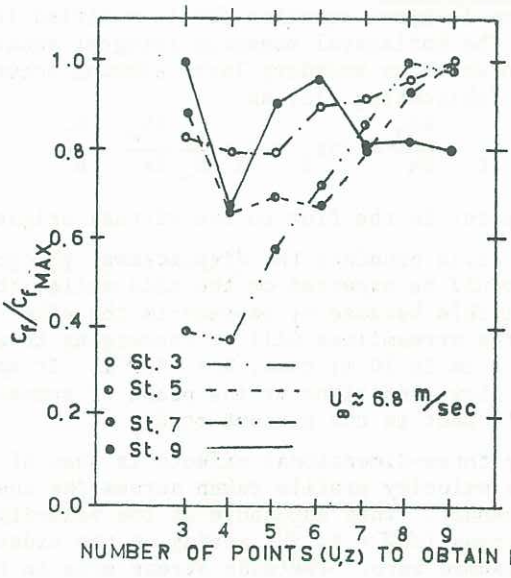

Fig. 3 - Sensitivity of Profile Shear Estimate to the Number of Points (U,y) Used

It has been demonstrated by many investigators (3,11) that the region, over a solid surface, of applicability of the 'law of the wall' (in part of which equation 7 applies) is roughly 0.1 to 0.2δ. Thus if the 'law of the wall' assumption is valid for an air-water boundary, it would be expected that equation 7 would be valid only in a similar region as for flow over a solid boundary. It is obvious that equation 7 has been assumed valid for a much larger region than allowed. Most investigators have assumed that the law of the wall extends as far as $z/\delta = 0.8$ as the velocity profile appears linear with log z in this region. Thus errors in this method must be expected.

Investigation of flow over a rough solid bound (6,8) have indicated that equation 7 should be modified to

$$\frac{U}{u_*} = \frac{1}{\kappa} \ln\left(\frac{z + E}{z_o}\right) \qquad (9)$$

where E is a distance which defines an origin for profiles that give the logarithmis distribution of velocity near the wall. In this study z is always located at the mean water surface and no attempt is made to determine E.

Applying the profile method in a region of $0.1 < z/\delta < 0.6$ ($z/\delta > 0.1$ is as close as the probes approach the surface) leads to an over-prediction of surface shear stress coefficient. A velocity profile from the results of Liu, et. al.(1966) demonstrates this fact effectively. They made a study of a turbulent boundary layer over rough walls and Fig. 4 shows one of their velocity profiles versus log z. The boundary layer thickness is approximately 2.5 in. The open circles represent the data before a correction to the z dimension is made and the solid circles represent the data with the z dimension corrected by E = 0.88 in. The regions $z/\delta \simeq 0.1$ and $z/\delta \simeq 0.6$ are marked on the figure. Even if the data is not corrected for zero shift, the region $0.1 < z/\delta < 0.6$ is fairly linear (dashed line); not having the information in the region $z/\delta < 0.1$ leads to a high estimate of the surface shear stress coefficient. This is generally the case for flow over a water surface. In the region $0.1 < z/\delta < 0.6$ the slope of the dashed curve is 23 percent higher than for the law of the wall region. Thus, if the profile method was applied to the data in this region the surface shear stress coefficient would be overpredicted by 52 percent. After z is corrected for zero displacement the region $0.15 < z/\delta < 0.6$ is again fairly linear (dashed line) and also leads to a high surface shear value. The actual law of the wall region is shown by the full line ($z/\delta < 0.2$) and the correct slope is obtained only after the z ordinate has been corrected for zero shift. It appears that velocity information is necessary to $z/\delta < 0.05$ to gain good profile results.

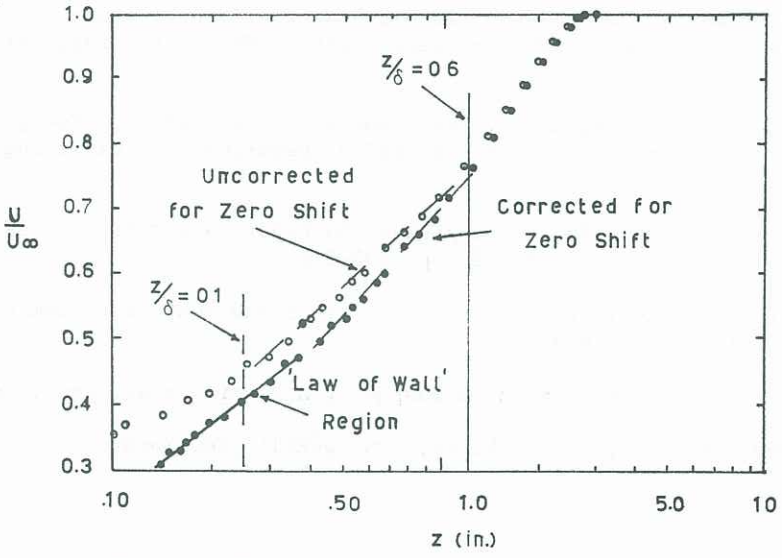

Fig. 4 - Velocity Profile Above a Rough Wall (from Liu, et. al., 1966, p. 43)

As the region to which the profile method is applied becomes further removed from the 'law of the wall' region ($z/\delta < 0.2$) one would expect that the predicted shear stress coefficients will overestimate the 'true' values by larger amounts. We see this in Figure 2: for $U_\infty \simeq 3.6$ m/sec the profile results are 1.5 times larger than the integral results, for $U_\infty \simeq 15.0$ m/sec this factor increases to 2.6. In Fig. 3 in all cases the ratio of $C_f/C_{f_{max}}$ tends to increase as the number of U,z data points to obtain C_f is increased from four to nine. This confirms the notion that the region of application of the law of the wall is incorrect.

The only way to extend the measurement region is by causing the velocity probe to follow the water surface in a manner similar to that described by Chang (2). It is of interest that Chang only reached a $z/\delta \simeq 0.1$, by oscillating the probe, for a wind speed $U_\infty \simeq 9$ m/sec. This indicates that not enough information is gained even by oscillating the velocity probe to obtain acceptable results using a profile method in a laboratory facility.

A further difficulty inherent in the use of a profile method is that two parameters must be obtained from the curve (slope and intercept). Priestly (9) compared wind stress values derived from wind profiles (over land) with simultaneous measurements of surface stress. Sufficient accuracy in the inferred results was not assured even though the measured values of U versus log z closely approximated a linear curve. Evidence was presented that values of shear stress of "acceptable" accuracy can be gained from the wind profile measurements only if z_0 is assigned in advance.

CONCLUSION

The main conclusion is that the profile method (Eq. 7) leads to overestimated values of the shear stress coefficient. The error becoming larger as the velocity is increased (Fig. 2). The authors feel (however, cannot justifiy) that the integral technique underpredicts the shear at the latter staions ($x > 9$ m). However, it is felt that the integral surface shear values are more consistent with the flow field than those given by the profile method.

ACKNOWLEDGMENTS

Support of the National Science Foundation under Grant GA-1471 is gratefully acknowledged.

APPENDIX 1 - REFERENCES

1. Chambers, A. J. P. A. Mangarella, R. L. Street, E. Y. Hsu (1970), "An experimental investigation of transfer of momentum at an air-water interface", Stanford University, Department of Civil Engineering, Tech. Rept. No. 133, Stanford.

2. Chang, P. C. (1968), "Laboratory measurements of air flow over wind waves following the moving water surface", Colorado State University, Colorado, Tech. Rept. CER68-69PcC18.

3. Hinze, J. E. (1959), Turbulence, McGraw-Hill, New York.

4. Hsu, E. Y. (1965), "A wind, water-wave research facility", Department of Civil Engineering, Stanford University, Tech. Rept. No. 57, Stanford.

5. Kays, W. M. (1966), Convective Heat and Mass Transfer, McGraw-Hill, Inc., New York.

6. Liu, C.K., S. J. Kline and J. P. Johnston (1966), "An experimental study of turbulent boundary layer on rough walls", Stanford University, Department of Mechanical Engineering, Tech. Rept. MD-15, Standford.

7. Mangarella, P. A., A. J. Chambers, R. L. Street and E. Y. Hsu (1971), "Energy and mass transfer through an air-water interface," Stanford University, Department of Civil Engineering, Tech. Rept. No. 134, Stanford.

8. Perry, A. E. and P. N. Joubert (1963), "Rough-wall boundary layers in adverse pressure gradients", J. Fluid Mech., Vol. 17, Pt. 2, pp. 193-211.

9. Priestly, C. H. B. (1959), "Estimation of surface stress and heat flux from profile data", Q. J. R. Met. Soc., Vol. 85, pp. 415-418.

10. Roll, H. U. (1965), Physics of the Marine Atmosphere, Academic Press, Inc., New York.

11. Schlichting, H. (1960), Boundary Layer Theory, McGraw-Hill, New York.